DNA-Damaging Enediyne C-1027 Inhibits Initiation of Intracellular SV40 DNA Replication in *trans*†

Mary M. McHugh,‡ Terry A. Beerman,*,‡ and William C. Burhans*,§

Department of Experimental Therapeutics and the Department of Molecular & Cellular Biology, Roswell Park Cancer Institute, Elm and Carlton Streets, Buffalo, New York 14263

Received August 22, 1996; Revised Manuscript Received October 23, 1996⊗

ABSTRACT: This study used 2-D agarose gel techniques to examine the effects of the DNA-strand scission enediyne C-1027 on DNA replication in SV40-infected BSC-1 cells. Replication of SV40 DNA was inhibited by C-1027 to a greater extent than was BSC-1 genomic DNA replication in infected cells. Low nanomolar concentrations (0.2−10 nM) of C-1027 affected a rapid, progressive decrease in SV40 replication activity and replication intermediates (RIs) within 15 min after drug addition. A concurrent decrease in the signal of both the SV40 bubble arc and replication activity with increasing concentrations of C-1027 suggested that C-1027 inhibited initiation of new RIs. Additionally, the reduction in bubble arc signal observed with C-1027 was prevented when elongation of nascent chains was blocked by aphidicolin. Thus, the C-1027-induced disappearance of RIs probably is related to the maturation of preformed replication molecules in the absence of initiation of new RIs. Strand damage to SV40 DNA was barely detectable at concentrations where inhibition of replication activity was nearly complete, indicating that C-1027 replication inhibition occurs in *trans*.

Enediyne drugs are potent antibiotics consisting of a protein moiety and a reactive chromophore which binds in the minor groove of DNA (Nicolaou et al., 1993a; Yu et al., 1995). DNA strand damage occurs when, under the appropriate conditions (e.g., the presence of thiols), the bound chromophore generates a benzenoid diradical (Nicolaou et al., 1992; Wrasidlo et al., 1995). The cytotoxicity of enediyne drugs is believed to be a consequence of chromophore-induced DNA damage (Nicolaou et al., 1992). An apoptotic mechanism may be involved in cell death (Corbeil et al., 1994; Jiang et al., 1995; Nicolaou et al., 1993b).

C-1027 is a recently discovered enediyne-chromophore containing agent (Hu et al., 1988; Yoshida et al., 1993) with unusually high cytotoxic activity against cultured cells (e.g., human KB and HL-60 cells and simian BSC-1 cells) and against certain murine tumors *in vivo* (e.g., L1210, P388, ascites hepatoma H22, sarcoma 180, and Harding−Passey melanoma) (McHugh et al., 1995; Zhen et al., 1989). While studies have confirmed C-1027 cytotoxicity is directly related to induction of DNA damage (Sugiura & Matsumoto, 1993; Xu et al., 1994), reports of specific effects on cell function are limited. Earlier studies showed that DNA synthesis in C-1027-treated cells was reduced to a greater extent than either RNA or protein synthesis (Sugimoto et al., 1990). Recently, this laboratory showed that both cytotoxicity and inhibition of DNA replication can be observed with picomolar doses of C-1027 (McHugh et al., 1995).

While C-1027 is a potent inhibitor of DNA replication, effects on specific molecular events in the replication process (i.e., initiation or elongation [or both] of nascent DNA chains) have not been reported. DNA electrophoresis on 2-D agarose gels can be used to determine the type and quantity of DNA replication intermediates (Brewer & Fangman, 1987; Cobuzzi et al., 1996; Snapka & Permana, 1993; Snapka et al., 1991a). Alterations in DNA migration patterns in 2-D gels can indicate whether agents which block DNA replication exert their inhibitory effect at the level of initiation or elongation of nascent DNA chains. Simian virus 40 (SV40) DNA replication provides a useful system for studying such effects, as parameters for its synthesis, both *in vitro* (using subcellular components) and *in vivo* (in infected cells) are well defined (Li & Kelly, 1984; Stillman et al., 1992; Tooze, 1980).

The present study examined the effects of dose and time of C-1027 exposure on DNA replication and induction of DNA damage in SV40-infected BSC-1 cells. DNA electrophoresis on 2-D gels was used to determine how C-1027 blocks SV40 DNA replication at different levels of DNA damage induction.

EXPERIMENTAL PROCEDURES

Chemicals. C-1027 was a generous gift of Dr. T. Otani (Taiho Pharmaceuticals Co., Ltd, Tokushima, Japan). Stock solutions were prepared in water and stored at −20 °C. [α-^{32}P]dCTP and GeneScreen membranes were obtained from Dupont NEN (Boston, MA). [^{3}H]TdR ([*methyl*-^{3}H]-thymidine, 48 Ci/mmol) was from CEA (France). DECAprime II DNA labeling kit was from Ambion (Austin, TX). Proteinase K was from Boehringer Mannheim (Indianapolis, IN). High-strength analytical grade agarose used for 2-D gels was obtained from Bio-Rad Laboratories (Hercules, CA). All other chemicals were reagent grade.

C-1027 Treatment of SV40-Infected BSC-1 Cells and Preparation of DNA. Maintenance of BSC-1 (African green

† This study was supported in part by Grants DHP-133 from the American Cancer Society, CA16056 from the National Cancer Institute, and MCB-9317011 from the National Science Foundation.

* To whom correspondence should be addressed. T.A.B. Tel: (716) 845-3443. FAX: (716) 845-8857. E-mail: Beerman@sc3101.med.buffalo.edu. W.C.B. Tel: (716) 845-7691. FAX: (716) 845-8169. E-mail: WBurhans@sc3101.med.buffalo.edu.

‡ Department of Experimental Therapeutics.

§ Department of Molecular & Cellular Biology.

⊗ Abstract published in *Advance ACS Abstracts,* December 15, 1996.

S0006-2960(96)02121-6 CCC: $14.00

monkey kidney) cells in Minimal Essential Medium plus 10% calf serum (MEM) and conditions for infection with the SV40 virus were described previously (Cobuzzi et al., 1996; Grimwade et al., 1987). Cells to be infected were plated at 5×10^5 per 100 mm plate and grown for 48 h until 80−90% confluent. Medium was removed, and cells were infected with SV40 virus in MEM containing 2% bovine calf serum (MEM-2). 2 h after infection, the virus-containing medium was replaced with 10 mL of virus-free MEM-2. 24 h after infection, 5 mL of medium was removed from each plate, and 25 μL of C-1027 at the appropriate concentration was added to the remaining 5 mL. For measurement of newly synthesized DNA, [^{3}H]TdR (10 μCi/mL of medium) was added during the last 30 min of the C-1027 incubation. Plates were rinsed three times with phosphate buffered saline (PBS), and cells were lysed by the addition of 3.0 mL of buffer A (100 mM EDTA, 1% sodium dodecyl sulfate [SDS], 0.2 mg/mL proteinase K). Plates were further incubated at 37 °C for 1h. Samples were divided into two aliquots: 0.5 mL was removed for forms analysis, and 2.5 mL was reserved for 2-D agarose gel electrophoresis.

2-D Gel Electrophoresis. Samples were prepared for 2-D gel electrophoresis by the addition, with mixing, of 1.04 mL of 4 M NaCl to 2.5 mL of sample. Samples were placed at 4 °C for 16 h, and centrifuged at 16 000 rpm in a Beckman SW-41 rotor for 30 min. The "Hirt" supernatant (Hirt, 1967) was extracted once with phenol and once with chloroform: isoamyl alcohol (24:1), precipitated with ethanol, resuspended in TE (10 mM Tris-HCl, pH 7.6, 1 mM ethylenediaminetetraacetic acid [EDTA]), and digested with the single-cut restriction enzyme *Bam*HI. Samples were assayed by neutral/neutral 2-D gel electrophoresis as described previously (Cobuzzi et al., 1996). Briefly, samples were electrophoresed on 0.6% agarose gels in 1× TAE, 0.1 μg/mL ethidium bromide for 24 h at 0.7 V/cm. Ethidium bromide stained DNA was visualized by placing the gel over an ultraviolet light source, and lanes were cut out and placed in a slot cut into the top of the second dimension gel (1% agarose) perpendicular to the direction of the current. The second-dimension gels were electrophoresed at 4 °C in 1× TBE, 0.5 μg/mL ethidium bromide for 19 h at 4 V/cm.

Forms Analysis. The 0.5 mL aliquot reserved for forms analysis was placed at 37 °C, mixed with 1% low gelling temperature agarose in PBS (sample:agarose = 4:1), and pipetted into the wells of a 1.0% agarose gel. After the samples solidified (15 min at 4 °C), the gel was placed in a submarine chamber containing 1× TAE and electrophoresed for 20 h at 1.5 V/cm. Addition of agarose to the sample was necessary to overcome the tendency of the SDS-containing cell lysate to float out of the wells of a submarine gel.

Southern Blots and Fluorography. All samples were electrophoresed in duplicate, and were either Southern blotted or processed for fluorography as described previously (Cobuzzi et al., 1996). Briefly, one gel was Southern blotted to GeneScreen and hybridized to [α-^{32}P]-radiolabeled full-length SV40 DNA. The DECAprime II DNA labeling kit was used for radiolabeling. The other gel was fluorographed by dehydration in ethanol (two washes in 95% ethanol for 1 h at room temperature), followed by soaking in absolute ethanol containing 5% 2,5-diphenyloxazole (PPO). After 1 h, the PPO/ethanol solution was removed and the gel was washed once for 1 h in H_2O to precipitate the fluors and then dried and exposed to X-ray film.

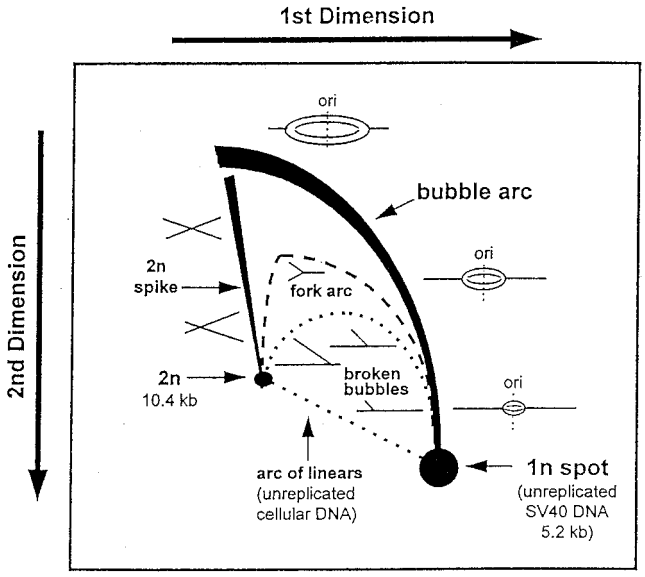

FIGURE 1: Migration patterns of RIs after electrophoresis in a typical 2-D neutral agarose gel. Conditions for electrophoresis are described in Experimental Procedures.

Quantitation. The quantity and distribution pattern of SV40 DNA on Southern blots was determined by exposing a phosphorimaging screen to the [α-^{32}P]-radiolabeled blots, then scanning the screen using a Molecular Dynamics Phosphorimager. For assaying replication activity, incorporation of [^{3}H]TdR into DNA was quantitated from X-ray films exposed to fluorographed gels and scanned using a Molecular Dynamics Densitometer. Both images were analyzed using ImageQuant software (Molecular Dynamics, Sunnyvale, CA). Changes in replication intermediates (RIs) on Southern blots were determined in ImageQuant by inserting identical ellipses over the tip of the bubble arc (BA) (i.e., to include the most intense signal in the upper left hand portion of the bubble arc), the 1*n* spot (1*n*) and over a portion of the blot in which no DNA was located (to provide a background value [BG]). It was important to use the same sized ellipse for quantitation of all samples within a single experiment, although the precise size of the ellipse did not matter. The volumes of the ellipses were quantitated and the bubble arc signal was calculated according to the formula

$$\text{BA signal} = \frac{\text{BA} - \text{BG}}{(1n - \text{BG})/(1n_{\text{control}} - \text{BG})}$$

where 1*n* and $1n_{\text{control}}$ refer to the amount of unreplicated *Bam*HI-linearized SV40 DNA in the sample and in the control, respectively (see diagram of 2-D gel in Figure 1).

Following electrophoresis in the first-dimension, gels were photographed over an ultraviolet light source using a Polaroid CU-5 Land Camera. Negatives from the Polaroid photographs were scanned and the amount of DNA in the linear FIII band quantitated with a densitometer. BA and BG were quantitated from the 2-D gels as described above. Replication activity (RA) was calculated according to the formula

$$\text{RA} = \frac{(\text{BA} - \text{BG})}{\text{FIII}/\text{FIII}_{\text{control}}}$$

where FIII and $\text{FIII}_{\text{control}}$ are the intensities on the first-

dimension gel of the ethidium bromide fluorescence of *Bam*HI-linearized SV40 DNA in the drug-treated sample and in the control, respectively.

RESULTS

Earlier studies from this laboratory described the ability of C-1027 to damage intracellular episomal, mitochondrial, and SV40 viral DNA targets (Cobuzzi et al., 1995; McHugh et al., 1995). The present study focused on C-1027-induced changes in replicating SV40 DNA 24 h after viral infection, when high levels of incorporation of [^{3}H]TdR into newly synthesized SV40 DNA are observed (Wang & Roman, 1981). C-1027 effects on SV40 DNA replication were examined using 2-D gel technology which is uniquely capable of separating replicating from nonreplicating DNA.

2-D Gel Analysis of Replication Intermediates (RIs)

Migration of RIs on 2-D Gels. SV40 DNA RIs were analyzed by neutral/neutral 2-D agarose gel electrophoresis using conditions described in Experimental Procedures. This technique separates molecules on the basis of size in the first dimension. In the second dimension, the nonlinear shape of replicating molecules alters their migration compared to linear non-replicating molecules. Figure 1 is a diagram of the typical distribution pattern of *Bam*HI restricted SV40 RIs on a 2-D gel after electrophoresis. SV40 replication occurs bidirectionally from the origin of replication. *Bam*HI cuts once within the termination region of SV40, at a point approximately opposite the origin of replication. Therefore, *Bam*HI restricted replicating molecules contain two replication forks equidistant from the origin of replication. In the second dimension gel, an arc ("bubble arc") consisting of a population of these molecules replicated to various extents, rises upward from the 1*n* spot, where linearized full-length non-replicating molecules of SV40 DNA migrate. In addition, smaller amounts of signal are associated with single forked molecules that correspond to bubble molecules in which one of the two forks is broken ("broken bubbles and fork arcs"). Fork breakage can occur when forks are destabilized in association with an inhibitory effect on nascent chain elongation, or during the isolation of DNA (Gilbert et al., 1995). Replicating and non-replicating DNA is visualized by Southern blotting and probing with SV40 sequences. In the present study, densitometric quantitation of the bubble arc signal and the 1*n* spot (see Experimental Procedures) indicated that 7%(±2% SEM) of the total intracellular SV40 DNA molecules were replicating at any given time.

C-1027 Concentration Effects on SV40 RIs. To determine drug doses optimal for examining effects on replication, SV40 RIs were assayed after infected BSC-1 cells were treated for 2 h with increasing concentrations of C-1027. For assay of replication activity, [^{3}H]TdR was added during the last 30 min of the C-1027 incubation. The replication activity and bubble arc signal of SV40 DNA on 2-D gels were determined by fluorography and by Southern blotting, respectively, as described in Experimental Procedures. Figure 2, panel A, shows a fluorogram and a Southern blot of representative SV40 RIs in a control and at two C-1027 dose points. In the fluorogram, the control (0 drug) sample had high levels of radiolabel associated both with the SV40 bubble arc and with BSC-1 genomic DNA (note the heavy line extending through the 1*n* and 2*n* spots). Fork arcs arise

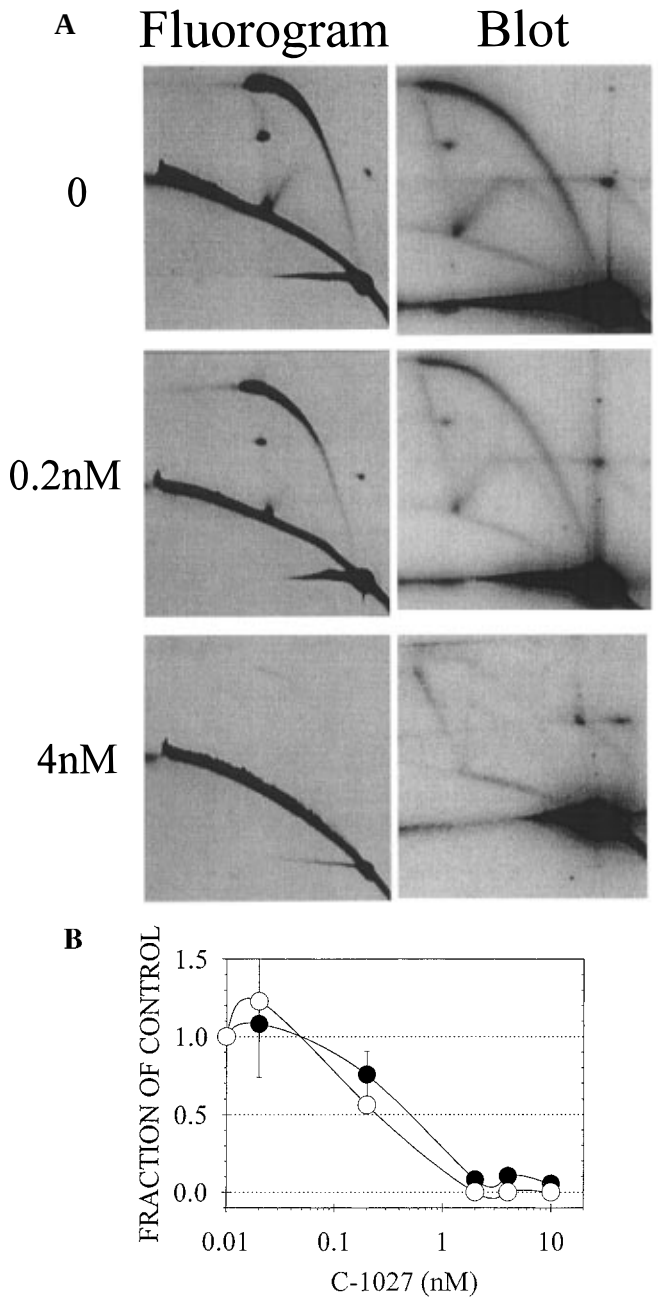

FIGURE 2: C-1027 concentration effects on SV40 replication activity and bubble arc signal. SV40 DNA from infected BSC-1 cells treated for 2 h with 0, 0.2 nM or 4nM C-1027 was electrophoresed on 2-D gels to separate RIs. (A) Duplicate samples assayed on a fluorogram and on a Southern blot. (B) Summary of changes in replication activity and signal of SV40 RIs with increasing C-1027 concentrations. Replication activity (○) and bubble arc signal (●) were quantitated by analysis of 2-D gel patterns as described in Experimental Procedures and divided by values from control samples to obtain the fraction of control shown on the *Y* axis. Data are from five experiments and are expressed ±SEM.

due to replication fork damage which occurs when elongation is inhibited (Cobuzzi et al., 1996; Gilbert et al., 1995). Such damage may be responsible for the presence of a faint fork arc in the 4 nM C-1027-treated samples. Incorporation of [^{3}H]TdR into the bubble arc, broken bubble arc, and fork arc was reduced in cells treated with 0.2 nM C-1027 and was undetectable with 4 nM C-1027.

Examination of duplicate samples by Southern blotting showed a similar progressive decrease in bubble arc signal with increasing C-1027 concentrations. In the control (0

drug) sample, a strong bubble arc signal, as well as a light arc corresponding to broken bubbles, was observed. The signals of both the bubble arc and the broken bubble arc were reduced with 0.2 nM C-1027 and were nearly undetectable with 4 nM C-1027. Since C-1027 is a DNA strand-scission agent, loss of signal could result simply from damage to the bulk of SV40 DNA which should be manifested by a decrease in the signal intensity of the 1*n* spot. However, increasing the C-1027 concentration had little effect on the signal of the 1*n* spot, indicating that C-1027 treatment caused a reduction in the fraction of SV40 molecules present as RIs, without significant damage to the total population of molecules.

Figure 2, panel B, summarizes the effect of increasing concentrations of C-1027 on SV40 replication activity and bubble arc signal detected by quantitation of fluorograms and Southern blots, respectively, as described in Experimental Procedures. Replication activity and bubble arc signal decreased over the drug range tested. For example, at 0.2 nM C-1027, the decrease in replication activity was 25% (±15% SEM) while bubble arc signal decreased by 44%-(±6% SEM).

Time Course of C-1027 Effects on SV40 RIs. As shown in Figure 2 above, a nearly complete loss of the bubble arc signal was observed after a 2 h treatment with 4 nM C-1027. Figure 3, panel A, shows a fluorogram and a Southern blot of representative SV40 RIs after incubation of infected cells with 4 nM C-1027 for 0, 15, or 60 min. The fluorogram shows incorporation of [^{3}H]TdR decreased within the first 15 min of C-1027 treatment. By 60 min, [^{3}H]TdR incorporation into SV40 RIs was undetectable. Visual inspection of the Southern blot showed that the bubble arc signal also progressively decreased with time. At 60 min, the bubble arc signal was very faint (bubble arc intensity was ≤5% that of the control bubble arc). Quantitation of fluorograms from several experiments confirmed a rapid decrease in replication activity with increasing time of exposure to C-1027 (Figure 3, panel B). Incorporation into RIs was reduced by 50% within 15 min, and was reduced by ≥90% after 30 min incubation with 4 nM C-1027.

Characterization of C-1027 Replication Inhibition. Comparison of changes in the number of RIs and in the incorporation of radiolabeled DNA precursors into these RIs can indicate whether treatments that inhibit DNA replication act at the level of initiation or elongation of nascent chains (Cobuzzi et al., 1996; Gilbert et al., 1995). Specific inhibition of initiation of DNA replication prevents the formation of new RIs but does not prevent the maturation of RIs formed before an initiation block has been established. Maturation of RIs in the absence of new initiation events results in a progressive decrease in the numbers of RIs, although the replication activity (i.e., elongation of nascent DNA chains) and incorporation of radioactive DNA precursors into preformed maturating molecules is not altered. Since initiation specific inhibition results in a decrease in the total number of RIs, a parallel decrease in the amount of incorporation of radiolabeled DNA precursors into the total population of RIs also is observed. By contrast, inhibition of nascent chain elongation does not result in substantial changes in the number of RIs, but incorporation of radioactive DNA precursors into individual RIs is reduced, and precursor incorporation into the total population of RIs is reduced to a greater extent than is the overall number of RIs.

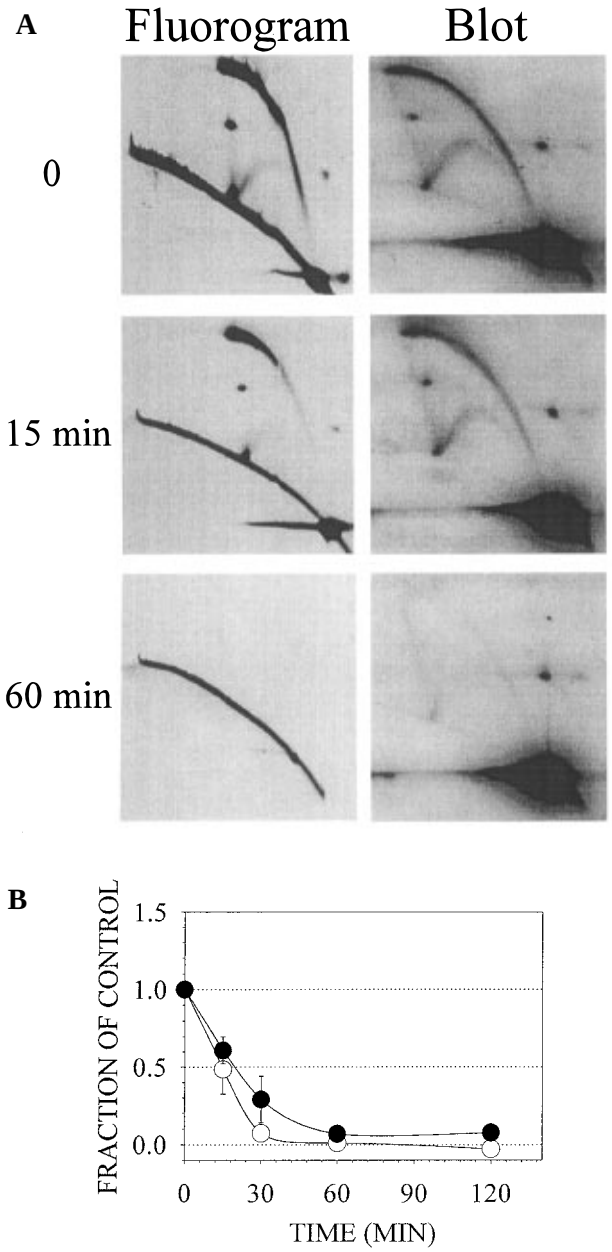

FIGURE 3: Time course of C-1027-induced changes in SV40 replication activity and bubble arc signal. SV40-infected BSC-1 cells were incubated with 4nM C-1027 for the times indicated. DNA was electrophoresed on 2-D gels. (A) Duplicate samples assayed on a fluorogram and on a Southern blot. (B) Summary of changes in the replication activity and bubble arc signal of SV40 when infected BSC-1 cells were incubated with 4 nM C-1027 for increasing periods of time. Replication activity (○) and bubble arc signal (●) were quantitated as described in Experimental Procedures. Data are from three experiments and are expressed ±SEM.

That C-1027 inhibits initiation of SV40 DNA replication was suggested by the data in Figures 2 and 3, which showed that the amount of SV40 RIs was decreased by C-1027 treatment. Although rapid destabilization of RIs by this strand scission agent might also account for the decrease in RIs, an increase in the gel fork and broken bubble arc signals associated with replication fork destabilization (Gilbert et al., 1995) was not observed. Additional evidence that C-1027 does not act by fork destabilization was obtained by assaying the effect of C-1027 in the presence of the well-documented elongation inhibitor, aphidicolin (Levenson &

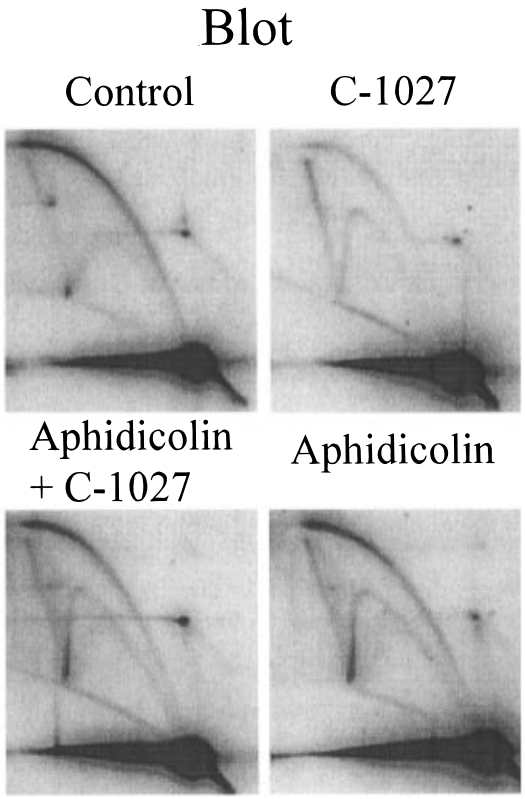

FIGURE 4: Aphidicolin inhibition of C-1027-induced loss of SV40 RI signal. SV40-infected BSC-1 cells were treated with 5 μM aphidicolin for 5 min prior to addition of 4 nM C-1027, and followed by further incubation for 2 h. Samples were electrophoresed on 2-D gels. A Southern blot of representative samples is shown.

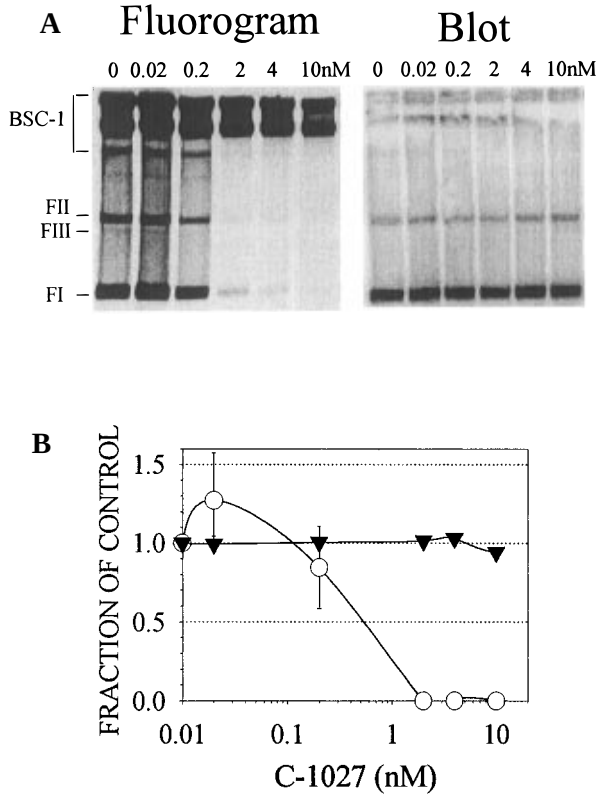

FIGURE 5: C-1027 concentration effects on [^{3}H]TdR incorporation and strand damage in total intracellular SV40 DNA. SV40-infected BSC-1 cells were incubated for 2 h with the C-1027 concentrations indicated. The position of SV40 forms I (FI), II (FII), and III (FIII) and of BSC-1 cell genomic DNA (BSC-1) are indicated. (A) Representative DNA samples analyzed on a fluorogram and on a Southern Blot. (B) Summary of C-1027 concentration effects on total [^{3}H]TdR incorporation into SV40 (sum of incorporation into FI, FII, and FIII), calculated from fluorograms, and expressed as a fraction of control incorporation (○). Southern blot determination of the ratio of form I to total SV40 DNA expressed as a fraction of the control ratio (▼). Data are from six experiments and are expressed ±SEM.

Hamlin, 1993; Snapka et al., 1991b; Wist, 1980). If SV40 RIs disappeared from C-1027-treated cells because they matured in the absence of new initiation events, aphidicolin's ability to inhibit elongation should block this maturation, and equal amounts of SV40 RIs should be observed in cells treated with both aphidicolin and C-1027 compared to those treated with aphidicolin alone. In contrast, C-1027 induced fork destabilization should cause SV40 RIs to disappear even when replication forks are first arrested by aphidicolin.

Figure 4 is a series of phosphorimages of Southern blots showing the effects on bubble arc signal of incubation with C-1027 in the absence and the presence of aphidicolin.

Treatment with 4 nM C-1027 alone reduced RIs in SV40 infected cells to 12% (±2% SEM) of control values (also see Figures 2 and 3), while substantial amounts of SV40 RIs were recovered from infected cells treated with both aphidicolin and C-1027 and with aphidicolin alone (77% [±8% SEM] and 67% [±11% SEM] of control values, respectively). These data indicate that the disappearance of most of the SV40 RIs in C-1027 treated cells was due to their maturation into fully replicated DNA. The decrease in SV40 RIs recovered from infected cells treated with aphidicolin alone compared to control cells may reflect a partial destabilization of replication forks (Gilbert et al., 1995; Snapka et al., 1991b), while the recovery of similar amounts of SV40 RIs from aphidicolin and C-1027 treated cells compared to those treated with aphidicolin alone demonstrated that C-1027 did not cause further destabilization of replication forks.

Comparison of C-1027 Effects on Replication Activity and DNA Strand Damage Using SV40 Forms Analysis. Forms analysis of SV40 DNA provided a simple method to determine the relationship between C-1027-induced changes in replication activity and induction of DNA strand damage. SV40 DNA from a crude cell lysate incubated with proteinase K was separated into supercoiled form I (FI), nicked circular form II (FII), and linear form III (FIII) by electrophoresis on agarose gels. In agreement with the results from 2-D gels presented in Figures 2−4, the fluorogram in Figure 5, panel A, shows a decrease in [^{3}H]TdR incorporation into SV40 DNA with ≥0.2 nM C-1027. Incorporation into all three SV40 forms (FI, II, and FIII) was drastically reduced with 2 and 4 nM, and was undetectable with 10 nM C-1027. By contrast, examination of the same samples on a Southern blot shows only a slight increase in FIII, indicative of strand damage, at the highest concentration of C-1027 tested (10 nM), and no change in the total amount of SV40 (forms I, II, and III, combined). Thus, the decreased incorporation of [^{3}H]TdR seen on the fluorogram was not due to a decrease in SV40 DNA in the C-1027 treated samples.

Data obtained from fluorograms and Southern blots are summarized in Figure 5, panel B. While only 2 nM C-1027 was required to inhibit replication of newly synthesized SV40 DNA by more than 95%, strand damage was barely detectable with 10 nM C-1027.

In Figure 5, panel A, the intense bands of high molecular weight DNA at the top of the fluorogram likely indicate incorporation of [^{3}H]TdR into newly synthesized BSC-1 genomic DNA, since no hybridization of [α-^{32}P]-radiolabeled SV40 was observed at the top of the Southern blot. By contrast with the SV40 results, incorporation into the high molecular weight BSC-1 genomic DNA was inhibited by less than 50% even at the highest concentration of C-1027 (10 nM). Since damage to BSC-1 genomic DNA cannot be quantitated using this type of analysis, the relationship between damage to BSC-1 genomic DNA and inhibition of replication activity was not determined.

DISCUSSION

Reports of drug effects on DNA replication previously relied on sucrose gradient analysis (Hatayama & Yukioka, 1983; Painter, 1986; Povirk & Goldberg, 1982) and usually involved the indirect analysis of newly replicated DNA by pulse-labeling techniques. The use of 2-D agarose gel techniques to distinguish between replicating and nonreplicating DNA on the basis of structure rather than incorporation of radiolabel was reported elsewhere (Friedman & Brewer, 1995; Huberman, 1994). The present study as well as an earlier report from this laboratory (Cobuzzi et al., 1996) used 2-D gel techniques to define how particular compounds that inhibit DNA replication exert their inhibitory effects.

That initiation of SV40 DNA synthesis is inhibited by C-1027 was indicated by the disappearance of the bubble arc signal (Figure 2 and 3). The decrease in RIs observed after C-1027 treatment also could be prevented by treatment with the elongation inhibitor, aphidicolin (see Figure 4). Moreover, under treatment conditions where decreases in the bubble arc signal are first detected, replication activity also decreases (Figures 2 and 3), indicating that elongation is not inhibited to a significant extent. In contrast, the elongation inhibitor, aphidicolin, completely inhibits replication activity while only a minimal effect on bubble arc signal is observed (Cobuzzi et al., 1996).

The related enediynes neocarzinostatin and auromomycin also reportedly inhibit initiation (Hatayama & Yukioka, 1983; Povirk & Goldberg, 1982). Other workers have reported initiation inhibition with a broad group of non-enediyne DNA reactive agents capable of inducing DNA damage, among them aflatoxin (Meneghini & Schumacher, 1977), 4-nitroquinoline 1-oxide, adriamycin, and ethyleneimine (Painter, 1978), daunomycin (Schellinx et al., 1979). Recently, this laboratory used 2-D gel analysis to show an inhibitory effect on SV40 replication initiation with the cyclopropylpyrroloindole DNA-alkylating agent adozelesin (Cobuzzi et al., 1996).

DNA damage reportedly is integral to the biological activity of enediynes (Hoffmann, 1993; Kagan et al., 1993; Nicolaou et al., 1993a) and likely is related to C-1027-induced replicative inhibition. However, the amount of SV40 DNA damage detected by forms analysis did not directly correspond to the extent of inhibition of SV40 replication. Single-strand damage was observed in $\leq$10% of the SV40 molecules at the highest concentration of C-1027 tested (10 nM) (see Figure 5), although replication activity was nearly completely inhibited with 4 nM C-1027 (see Figures 2−4).

Although selective targeting of replicating DNA is a possible explanation for the difference in C-1027 concentrations required for detection of DNA strand damage and replication inhibition, it probably does not account for initiation inhibition at low levels of DNA damage. For example, if damage induction is linear, $\leq$0.4% of SV40 molecules should be damaged at 0.5 nM C-1027, which affects a 50% reduction in SV40 replication activity. In the present study, 7% ($\pm$2% SEM) of total intracellular SV40 molecules exist as replication intermediates. Even if all damage was localized to replicating DNA, only a small fraction of replicating molecules (0.4% compared to 7%) would be damaged at a concentration where substantial inhibition of replication activity is observed. Thus, selective targeting of replicating DNA as a mechanism for replicative inhibition at picomolar concentrations of C-1027 is unlikely.

Some fraction of the replication inhibition may reflect damage to replicating DNA at higher C-1027 concentrations. Forms analysis shows that 4 nM C-1027 should induce damage in $\leq$4% of SV40 molecules. If damage is limited to replicating molecules, approximately one-half of all replicating molecules (7% of total SV40, see above) would be affected. However, how C-1027 might distinguish between replicating and non-replicating SV40 DNA is unclear.

That C-1027 may affect elongation as well as initiation has not been ruled out. Although marginal, differences between C-1027-induced decreases in the amount of RIs and replication activity may be real (Figures 2B and 3B). The pattern observed with higher C-1027 concentrations (i.e., less effect on the amount of RIs than on the replication activity) would be consistent with blockage of elongation. The fork and broken bubble signals observed in DNA from cells treated with higher concentrations of drug (e.g., 4nM C-1027) also suggested a partial elongation block. Both the strand-scission enediyne neocarzinostatin and the alkylating agent adozelesin reportedly inhibit elongation at higher concentrations (Cobuzzi et al., 1996; Hatayama & Yukioka, 1983). Thus, although enediynes and alkylating agents differ in the type of DNA lesion induced, effects on DNA replication may be similar.

In infected cells, SV40 DNA synthesis was inhibited by C-1027 to a greater extent than was BSC-1 cell genomic DNA synthesis. These differences may relate to the amount of DNA damage induced. We previously showed that C-1027 induced 40-fold more strand damage in SV40 DNA in infected cells than in genomic DNA from uninfected BSC-1 cells (McHugh et al., 1995). Because of size differences between SV40 and cellular replicons, differing times are required to complete their replication. *In vivo*, SV40 replication proceeds from a single origin at a rate of 145 base pairs per minute per replication fork (Tapper et al., 1979), and one round of SV40 replication (i.e., initiation and elongation to fully mature SV40 molecules) should be completed within approximately 36 min. Thus, during the 30−60 min that C-1027 is active, elongation of SV40 has been completed and, if C-1027 inhibits initiation, no new RIs have been initiated, resulting in a measurable decrease in replication activity. By contrast, the larger sized genomic replicons can continue to elongate and incorporate [^{3}H]TdR even if new initiation events are inhibited.

Low levels of C-1027-induced damage appear to inhibit initiation of SV40 DNA by a *trans* effect. While it is not known whether other enediyne agents inhibit replication in a similar fashion, such a *trans*-acting mechanism was

reported recently with adozelesin, a DNA alkylating agent (Cobuzzi et al., 1996). Both adozelesin and C-1027 inhibit replication rapidly (within 15−30 min after drug addition). Since both drugs share a preference for AT rich sequences (Lee et al., 1994; Sugiura & Matsumoto, 1993), the *trans* induced inhibitory effect may relate to the induction of damage to a cellular gene which is necessary for initiation of DNA replication. Alternatively, the inhibitory effect on SV40 replication may occur as part of a cellular response to damage anywhere in the genome, and would be independent of the type of DNA damage since C-1027 causes direct DNA double-strand breaks while adozelesin induces adducts within the DNA minor groove (Li et al., 1991; Smith et al., 1995).

The inhibitory effect on initiation triggered by C-1027 and other DNA damaging agents could be mediated as part of a checkpoint regulatory pathway that protects cells from the deleterious consequences of DNA damage by arresting DNA replication. Although most checkpoint responses that have been characterized previously occur outside of S phase**,** a transient arrest of DNA synthesis within S phase has been reported with a variety of DNA damaging agents (Kaufmann, 1995). For adozelesin, a kinase-dependent mechanism has been suggested by Bhuyan and colleagues (Bhuyan et al., 1992a,b) who demonstrated that adozelesin effects the cell cycle by transiently inhibiting progression through S-phase followed by long-term G_2 arrest. An intra-S phase checkpoint response to DNA damage partially mediated by the *MEC1* gene, which is structurally similar to the human *ATM* gene, mutations in which are associated with ataxia telangiectasia, was recently described in yeast (Paulovich & Hartwell, 1995). Future studies will identify the mechanism responsible for the *trans*-induced blockage of replication at the level of initiation and will explore whether other enediynes behave similarly to C-1027.

REFERENCES

Bhuyan, B. K., Smith, K. S., Adams, E. G., Petzold, G. L., & McGovren, J. P. (1992a) *Cancer Res. 52*, 5687−5692.

Bhuyan, B. K., Smith, K. S., Adams, E. G., Wallace, T. L., Von Hoff, D. D., & Li, L. H. (1992b) *Cancer Chemother. Pharmacol. 30*, 348−354.

Brewer, B. J., & Fangman, W. L. (1987) *Cell 51*, 463−471.

Cobuzzi, R. J., Jr., Kotsopoulos, S. K., Otani, T., & Beerman, T. A. (1995) *Biochemistry 34*, 583−592.

Cobuzzi, R. J., Burhans, W. C., & Beerman, T. A. (1996) *J. Biol. Chem. 271*, 19852−19859.

Corbeil, J., Richman, D. D., Wrasidlo, W., Nicolaou, K. C., & Looney, D. J. (1994) *Cancer Res. 54*, 4270−4273.

Friedman, K. L., & Brewer, B. J. (1995) in *DNA Replication* (Campbell, J. L., Ed.) pp 613−627, Academic Press, Inc., New York.

Gilbert, D. M., Neilson, A., Miyazawa, H., DePamphilis, M. L., & Burhans, W. C. (1995) *J. Biol. Chem. 270*, 9597−9606.

Grimwade, J. E., Cason, E. B., & Beerman, T. A. (1987) *Nucleic Acids Res. 15*, 6315−6329.

Hatayama, T., & Yukioka, M. (1983) *Biochim. Biophys. Acta 740*, 291−299.

Hirt, B. (1967) *J. Mol. Biol. 26*, 365−369.

Hoffmann, R. (1993) *Am. Sci. 81*, 324−326.

Hu, J. L., Xue, Y. C., Xie, M. Y., Zhang, R., Otani, T., Minami, Y., Yamada, Y., & Marunaka, T. (1988) *J. Antibiotics 41*, 1575−1579.

Huberman, J. A. (1994) in *The Cell Cycle: A Practical Approach* (Fantes, P., & Brooks, R. F., Eds.) pp 213−234, Oxford University Press, Oxford

Jiang, B., Li, D. D., & Zhen, Y. S. (1995) *Biochem. Biophys. Res. Commun. 208*, 238−244.

Kagan, J., Wang, X., Chen, X., Lau, K. Y., Batac, I. V., Tuveson, R. W., & Hudson, J. B. (1993) *J. Photochem. Photobiol. B: Biol. 21*, 135−142.

Kaufmann, W. K. (1995) *Cancer Metastasis Rev. 14*, 31−41.

Lee, C. S., Pfeifer, G. P., & Gibson, N. W. (1994) *Biochemistry 33*, 6024−6030.

Levenson, V., & Hamlin, J. L. (1993) *Nucleic Acids Res. 21*, 3997−4004.

Li, J. J., & Kelly, T. J. (1984) *Proc. Natl. Acad. Sci. U.S.A. 81*, 6973−6977.

Li, L. H., Kelly, R. C., Warpehoski, M. A., McGovren, J. P., Gebhard, I., & DeKoning, T. F. (1991) *Invest. New Drugs 9*, 137−148.

McHugh, M. M., Woynarowski, J. M., Gawron, L. S., Otani, T., & Beerman, T. A. (1995) *Biochemistry 34*, 1805−1814.

Meneghini, R., & Schumacher, R. I. (1977) *Chem.−Biol. Interact. 18*, 267−276.

Nicolaou, K. C., Dai, W. M., Tsay, S. C., Estevez, V. A., & Wrasidlo, W. (1992) *Science 256*, 1172−1178.

Nicolaou, K. C., Smith, A. L., & Yue, E. W. (1993a) *Proc. Natl. Acad. Sci. U.S.A. 90*, 5881−5888.

Nicolaou, K. C., Stabila, P., Esmaeli-Azad, B., Wrasidlo, W., & Hiatt, A. (1993b) *Proc. Natl. Acad. Sci. U.S.A. 90*, 3142−3146.

Painter, R. B. (1978) *Cancer Res. 38*, 4445−4449.

Painter, R. B. (1986) *Int. J. Radiat. Biol. Relat. Studies Phys. Chem. Med. 49*, 771−781.

Paulovich, A. G., & Hartwell, L. H. (1995) *Cell 82*, 841−847.

Povirk, L. F., & Goldberg, I. H. (1982) *Biochemistry 21*, 5857−5862.

Schellinx, J. A., Dijkwel, P. A., & Wanka, F. (1979) *Eur. J. Biochem. 102*, 409−416.

Smith, K. S., Folz, B. A., Adams, E. G., & Bhuyan, B. K. (1995) *Cancer Chemother. Pharmacol. 35*, 471−482.

Snapka, R. M., & Permana, P. A. (1993) *BioEssays 15*, 121−127.

Snapka, R. M., Permana, P. A., Marquit, G., & Shin, C.-G. (1991a) *Methods: A Companion to Methods in Enzymology*, Vol. 3, No. 2, pp 73, Academic Press, San Diego, CA.

Snapka, R. M., Shin, C. G., Permana, P. A., & Strayer, J. (1991b) *Nucleic Acids Res. 19*, 5065−5072.

Stillman, B., Bell, S. P., Dutta, A., & Marahrens, Y. (1992) *Ciba Found. Symp. 170*, 147−156, discussion pp 156−160.

Sugimoto, Y., Otani, T., Oie, S., Wierzba, K., & Yamada, Y. (1990) *J. Antibiotics 43*, 417−421.

Sugiura, Y., & Matsumoto, T. (1993) *Biochemistry 32*, 5548−5553.

Tapper, D. P., Anderson, S., & DePamphilis, M. L. (1979) *Biochim. Biophys. Acta 565*, 84−97.

Tooze, S. (1980) *Molecular Biology of Tumor Viruses*, Part 2, 2nd ed., Cold Spring Harbor Laboratory, Inc., Plainview, NY.

Wang, H. T., & Roman, A. (1981) *J. Virol. 39*, 255−262.

Wist, E. (1980) *Experientia 36*, 405−406.

Wrasidlo, W., Hiatt, A., Mauch, S., Merlock, R. A., & Nicolaou, K. C. (1995) *Acta Oncol. 34*, 157−164.

Xu, Y. J., Zhen, Y. S., & Goldberg, I. H. (1994) *Biochemistry 33*, 5947−5954.

Yoshida, K.-I., Minami, Y., Azuma, R., Saeki, M., & Otani, T. (1993) *Tetrahedron Lett. 34*, 2637−2640.

Yu, L., Mah, S., Otani, T., & Dedon, P. (1995) *J. Am. Chem. Soc. 117*, 8877−8878.

Zhen, Y. S., Ming, X. Y., Yu, B., Otani, T., Saito, H., & Yamada, Y. (1989) *J. Antibiot. 42*, 1294−1298.

BI962121A